the reduced gradient bubble model and phase mechanics

by Dr. Bruce Weinke

Modeling of decompression phenomena in the body is a difficult task, and existing models are incomplete at best. With these caveats, models and underpinning physical principles of decompression are the focus of this article. Free and dissolved gas phases, and transfer mechanisms are pinpointed. Differences between dissolved and free phase models are contrasted.

Introduction

Modeling of decompression phenomena in the human body is, at times, more of an artform than a science. Some take the view that deterministic modeling can only be fortuitous. Technological advance, elucidation of competing mechanisms, and resolution of model issues over the past 80 years has not been rapid. Model applications tend to be ad hoc, tied to data fits, and difficult to quantify on first principles. Almost any description of decompression processes in tissue and blood can

Sea Level Surfacing Ratios and Critical Tensions

halftime τ (min)	Critical Ratio R_0	Critical Tension M_0 (fsw)	Tension Change ΔM
5	3.15	104	2.27
10	2.67	88	2.01
20	2.18	72	1.67
40	1.76	58	1.34
80	1.58	52	1.26
120	1.55	51	1.19

Table 1—Sea Level Surfacing Ratios and Critical Tensions

Critical Phase Volume Time Limits

Depth d (fsw)	Nonstop Limit t_n (min)	Depth d (fsw)	Nonstop Limit t_n (min)
30	250	130	9
40	130	140	8
50	73	150	7
60	52	160	6.5
70	39	170	5.8
80	27	180	5.3
90	22	190	4.6
100	18	200	4.1
110	15	210	3.7
120	12	220	3.1

Table 2—Critical Phase Volume Time Limits

Critical Phase Volume Gradients

halftime τ (min)	Threshold Depth δ (fsw)	Surface Gradient G_0 (fsw)	Gradient Change ΔG
2	190	151	.518
5	135	95	.515
10	95	67	.511
20	65	49	.506
40	40	36	.468
80	30	27	.417
120	28	24	.379
240	16	23	.329
480	12	22	.312

Table 3—Critical Phase Volume Gradients

be disputed, and turned around on itself. The fact that decompression takes place in metabolic and perfused matter makes it difficult to design and analyze experiments outside living matter. Yet, for application to safe diving, we need models to build tables and meters. And deterministic models, not discounting shortcomings, are the subject of this discourse.

MODELS

Most believe that the pathophysiology of decompression sickness syndrome follows formation of a gas phase after decompression. Yet, the physiological evolution of the gas phase is poorly understood. Bubble detection technology has established that moving and stationary bubbles do occur following decompression, that the risk of decompression sickness increases with the magnitude of detected bubbles, that symptomless, or silent, bubbles are also common following decompression, and that the variability in gas phase formation is less likely than the variability in symptom generation. Taken together, gas phase formation is not only important to the understanding of decompression sickness, but is also a crucial model element in theory and computation.

Bubbles can form in tissue and blood when ambient pressure drops below tissue tensions, according to dissolved-free phase mechanics. Trying to track free and dissolved gas buildup and elimination in tissue and blood, especially their interplay, is extremely complex, beyond the capabilities of today's supercomputers. But safe computational prescriptions are necessary in the formulation of dive tables and digital meter algorithms. The simplest way to stage decompression, following extended exposures to high pressure with commensurate dissolved gas buildup, is to limit tissue tensions. Historically, Haldane first employed the approach, and it persists today in modified form.

History

Tables and schedules for diving at sea level can be traced to a model proposed in 1908 by the eminent English physiologist, John Scott Haldane. He observed that goats, saturated to depths of 165 feet of sea water (fsw), did not develop decompression sickness (DCS) if subsequent decompression was limited to half the ambient pressure. Extrapolating to humans, researchers reckoned that tissues tolerate elevated dissolved gas pressures (tensions), greater than ambient by a factor of two, before the onset of DCS symptoms. Haldane then constructed schedules which limited the critical supersaturation ratio to two in hypothetical tissue compartments. Tissue compartments were characterized by their halftime, τ. Halftime is also termed half-life when linked to exponential

processes, such as radioactive decay. Five compartments (5, 10, 20, 40, and 75 minutes) were employed in decompression calculations and staged procedures for fifty years.

Some years following, in performing deep diving and expanding existing table ranges in the 1930s, U.S. Navy investigators assigned separate limiting tensions (M-values) to each tissue compartment. Later in the 1950s and early 1960s, other US Navy investigators, in addressing repetitive exposures for the first time, advocated the use of six tissues (5, 10, 20, 40, 80, and 120 minutes) in constructing decompression schedules, with each tissue compartment again possessing its own limiting tension. Temporal uptake and elimination of inert gas was based on mechanics addressing only the macroscopic aspects of gas exchange between blood and tissue. Exact bubble production mechanisms, interplay of free and dissolved gas phases, and related transport phenomena were not quantified, since they were neither known nor understood. Today, we know much more about dissolved and free phase dynamics, bubbles, and transport mechanisms, but still rely heavily on the Haldane model. Inertia and simplicity tend to sustain its popularity and use, and it has been a workhorse.

To maximize the rate of uptake or elimination of dissolved gases, the gradient is maximized by pulling the diver as close to the surface as possible. Exposures are limited by requiring that the tissue tensions never exceed limits (called M-values), for instance, written for each compartment in the US Navy approach (5, 10, 20, 40, 80, and 120 minute tissue halftimes) τ, as, $M = M_0 + \Delta M d$, with, $M_0 = 152.7\tau^{-1/4}$, and, $\Delta M = 3.25\tau^{-1/4}$, as a function of depth, d; for ΔM the change per unit depth. Obviously, M, is largest for fast tissue compartments (τ small), and smallest for slow tissue compartments (τ large). Fast compartments control short deep excursions, while slow compartments control long shallow excursions. Surfacing values, M_0, are principal concerns in nonstop diving, while values at depth, $\Delta M d$, concern decompression diving. In both cases, the staging regimen tries to pull the diver as close to the surface as possible, in as short a time as possible. By contrast, free phase (bubble) elimination gradients, as seen, increase with depth, directly opposite to dissolved gas elimination gradients which decrease with depth. In actuality, decompression is a playoff between dissolved gas buildup and free phase growth, tempered by body ability to eliminate both. But dissolved gas models cannot handle both, so there are problems when extrapolating outside tested ranges.
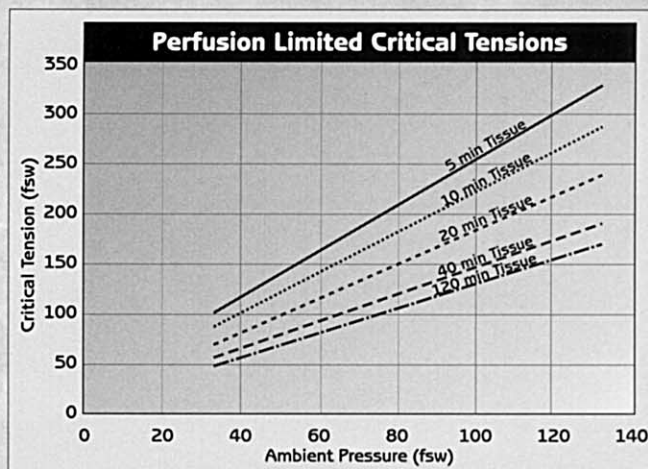
(continued next page)

Figure 1—Critical tensions are linear functions of pressure in the Haldane scheme, obviously increasing with ambient pressure. Faster compartments permit larger amounts of dissolved nitrogen, slower compartments less.
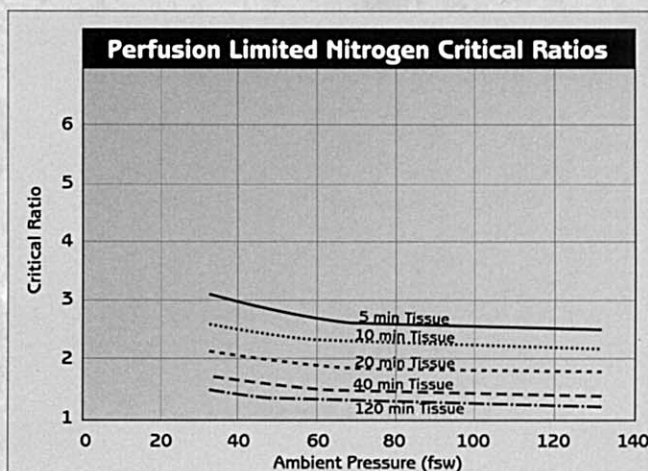

Figure 2—Critical ratios, R, are simply the critical tensions, M, divided by the ambient pressure, P, and are seen to be hyperbolic functions of pressure. Faster compartments support larger critical ratios, and slower compartments smaller critical ratios.
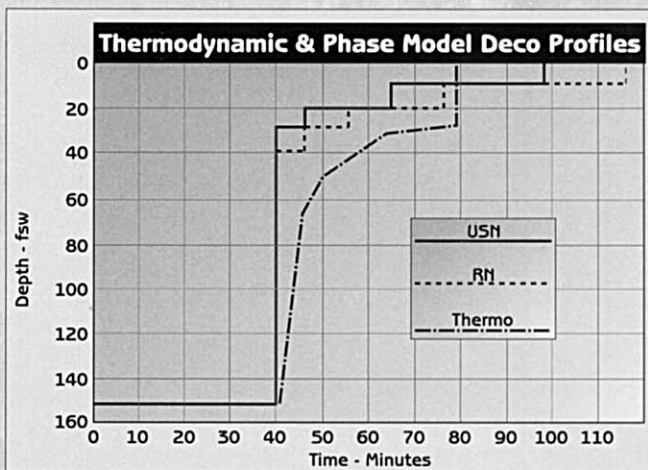

Figure 3—Decompression profiles for a dive to 150 fsw for 40 minutes are depicted according to supersaturation and phase decompression formats. Differences between supersaturation schedules (USN and RN) and the phase format schedule (thermo) are generic to bubble models vs. critical tension models, and are based on the fundamental differences between eliminating free and dissolved gas phases. Decompression staging is a playoff in trying to eliminate both.
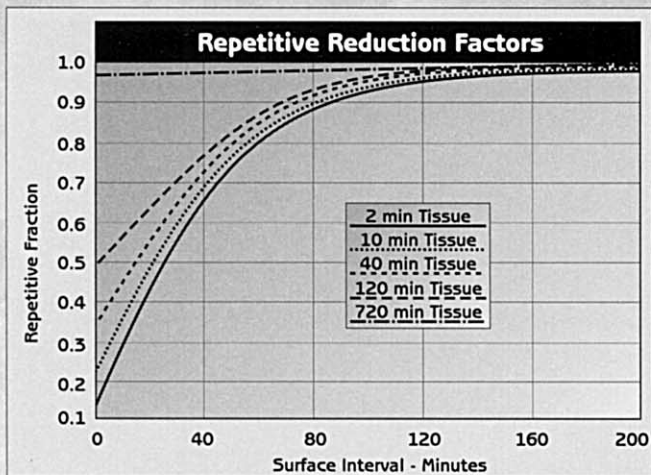
Repetitive Reduction Factors

Figure 4—Within the phase volume constraint, bubble elimination periods are shortened over repetitive diving, compared to bounce diving. Faster compartments are impacted the most, but all fractions relax to one after a few hours.
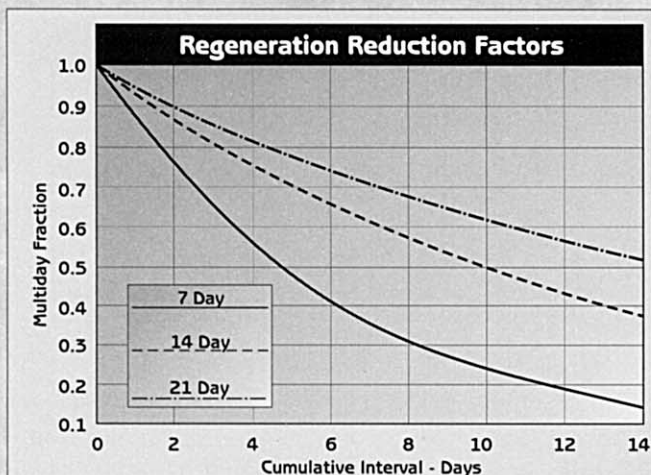
Regeneration Reduction Factors

Figure 5—Micronuclei are thought to regenerate over adaptation time scales (days), replenishing existing pools of gas seeds. A factor η^{res}, accounting for creation of new micronuclei, reduces permissible gradients by the creation rate, thus maintaining the phase volume constraint over multiday diving.
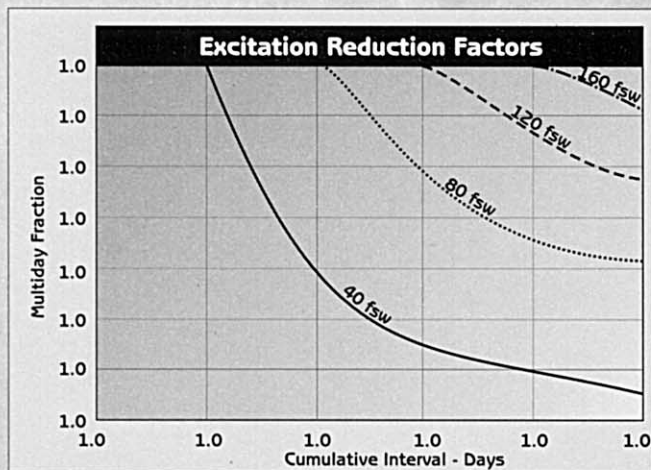
Excitation Reduction Factors

Figure 6—Deeper-than-previous diving activity stimulates smaller bubble seeds into growth according to the varying permeability and reduced gradient bubble models. Scaling gradients by the ratio of bubble excess on the deepest points of earlier dives, η^{exc}, maintains the phase volume constraint for multidiving. Shallow dives followed by deeper dives incur the largest reductions in permissible gradients.

32

A popular set of (surfacing) critical tensions, M_o, and corresponding critical ratios, $R_o = M_o / P_o$, and changes per foot of depth, ΔM, are listed in Table 1 under appropriate headings. Critical parameters, according to the U.S. Navy, are also plotted in Figures 1 and 2. In absolute pressure units, the corresponding critical gradient, $G = Q - P$, is related to ambient pressure, P, and critical nitrogen pressure, M, with, $Q = 1.27 M$. In bubble theories, supersaturation is limited by the critical gradient, G. In decompressed gel experiments, Strauss suggested that G 20 fsw at ambient pressures less than a few atmospheres. Other studies suggest, 14 G 30 fsw , as a range of critical gradients (G-values). In diffusion-dominated approaches, the tissue tension can be limited by a single, pressure criterion, such as, $M = 709P / P + 404$.

Blood rich, well-perfused, aqueous tissues are usually thought to be fast (small τ), while blood poor, scarcely-perfused, lipid tissues are thought to be slow (large τ), though the spectrum of halftimes is not correlated with actual perfusion rates in critical tissues. As reflected in relationship above, critical parameters are obviously larger for faster tissues. The range of variation with compartment and depth is not insignificant. Fast compartments control short deep exposures, while slow compartments control long shallow, decompression, and saturation exposures.

Multitissue Model

Multitissue models, variations of the original Haldane model, assume that dissolved gas exchange, controlled by blood flow across regions of varying concentration, is driven by the local gradient, that is, the difference between the arterial blood tension and the instantaneous tissue tension. Tissue response is modeled by exponential functions, bounded by arterial and initial tensions, and perfusion constants, lambda , linked to the tissue halftimes, τ, for instance, 1, 2, 5, 10, 20, 40, 80, 120, 180, 240, 360, 480, and 720 minute compartments assumed to be independent of pressure.

In a series of dives or multiple stages, initial and arterial tensions represent extremes for each stage, or more precisely, the initial tension and the arterial tension at the beginning of the next stage. Stages are treated sequentially, with finishing tensions at one step representing initial tensions for the next step, and so on. To maximize the rate of uptake or elimination of dissolved gases the gradient, simply the difference between arterial and tissue tensions is maximized by pulling the diver as close to the surface as possible. Exposures are limited by requiring that the tissue tensions never exceed $M = M_o + \Delta Md$, as a function of depth, d, for ΔM the change per unit depth. A set of M_o and ΔM are listed in Table 1.

At altitude, some critical tensions have been correlated with actual testing, in which case, an effective depth, d = P - 33, is referenced to the absolute pressure, P, with surface pressure, P_h = 33 exp (-0.0381 h), at elevation, h, and h in multiples of 1,000 ft. However, in those cases where critical tensions have not been tested, nor extended, to altitude, an exponentially decreasing extrapolation scheme, called similarity, has been employed. Extrapolations of critical tensions, below P = 33 fsw, then fall off more rapidly then in the linear case. A similarity extrapolation holds the ratio, R = M/P, constant at altitude. Estimating minimum surface tension pressure of bubbles near 10 fsw, as a limit point, the similarity extrapolation might be limited to 10,000 ft in elevation, and neither for decompression nor heavy repetitive diving.

Models of dissolved gas transport and coupled bubble formation are not complete, and all need correlation with experiment and wet testing. Extensions of basic (perfusion and diffusion) models can redress some of the difficulties and deficiencies, both in theory and application. Concerns about microbubbles in the blood impacting gas elimination, geometry of the tissue region with respect to gas exchange, penetration depths for gas diffusion, nerve deformation trigger points for pain, gas uptake and elimination asymmetry, effective gas exchange with flowing blood, and perfusion versus diffusion limited gas exchange, to name but a few, motivate a number of extensions of dissolved gas models.

The multitissue model addresses dissolved gas transport with saturation gradients driving the elimination. In the presence of free phases, free-dissolved and free-blood elimination gradients can compete with dissolved-blood gradients. One suggestion is that the gradient be split into two weighted parts, the free blood and dissolved-blood gradients, with the weighting fraction proportional to the amount of separated gas per unit tissue volume. Use of a split gradient is consistent with multiphase flow partitioning, and implies that only a portion of tissue gas has separated, with the remainder dissolved. Such a split representation can replace any of the gradient terms in tissue response functions.

If gas nuclei are entrained in the circulatory system, blood perfusion rates are effectively lowered, an impairment with impact on all gas exchange processes. This suggests a possible lengthening of tissue halftimes for elimination over those for uptake, for instance, a 10 minute compartment for uptake becomes a 12 minute compartment on elimination. Such lengthening procedure and the split elimination gradient obviously render gas uptake and
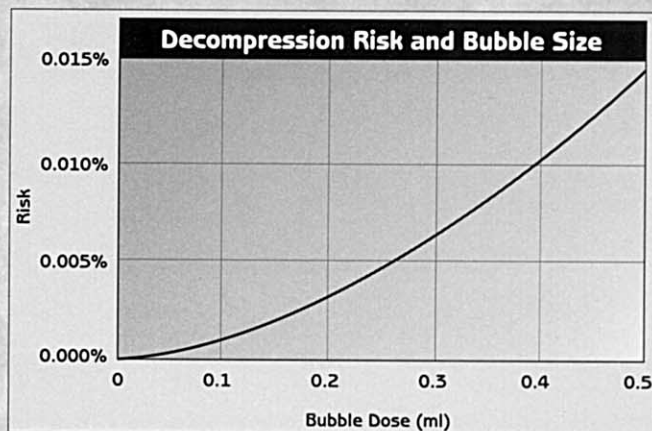
Figure 7—It is possible to correlate model parameters with experimental diving data. The above relationship correlates risk with computed model bubble size, that is, theoretically computed bubble dose (ml) is linked to incidence of decompression sickness in the sigmoidal dose curve. Dose is a measure of separated gas volume, a natural trigger point in phase models.
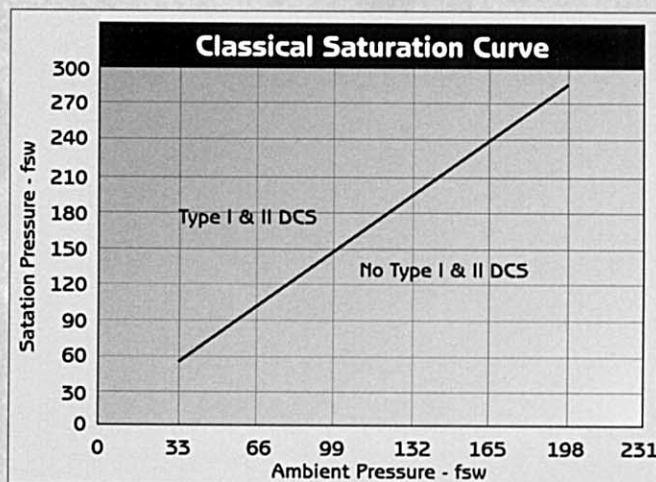

Figure 8—The classical saturation curve relates saturated tissue tension, Q, to permissible pressure on decompression, P, in linear fashion with, Q = 1.37P + 11.1, holding in the hyperbaric region, P 33 fsw , but questionable in the hypobaric region, P < 33 fsw, especially as P drops below 16 fsw.
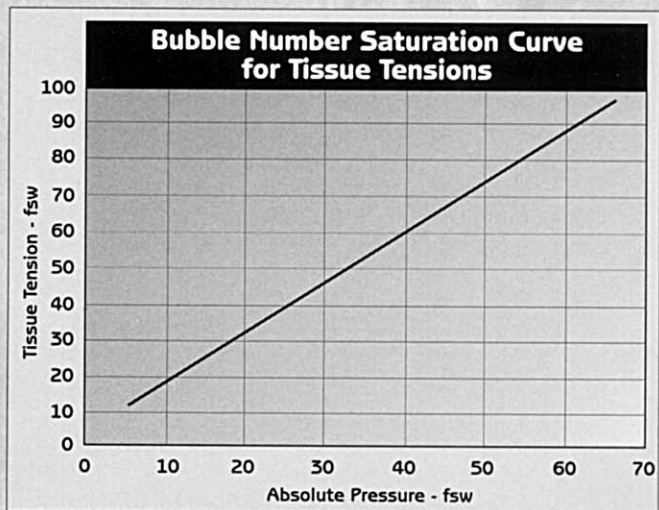

Figure 9—In exponentially decreasing bubble size models, such as the VPM and RGBM, with excitation radii inversely proportional to compression-decompression pressures, the saturated tissue tension, Q, in absolute units satisfies, Q = [2.31 - exp(-11.3/P)]P, exhibiting a linear behavior for large P, and passing through the origin as P approaches zero. The curve thus possesses the desired hyperbaric and hypobaric form across a broad pressure range.
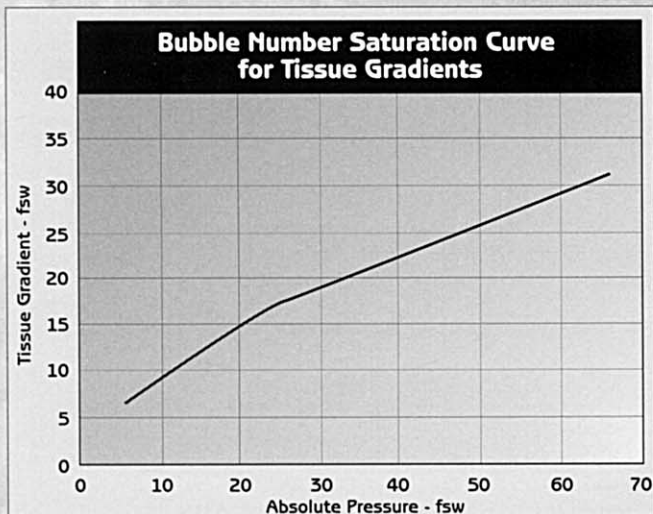
Bubble Number Saturation Curve for Tissue Gradients

Figure 10—In analogy with the tension, the saturated tissue gradient, G, exhibits similar behavior, Permissible saturation gradient, G, is given by, $G = [1.31 - \exp(-11.3/P)]P$, another curve approximating a straight line for large P, and passing through the origin as P gets small.
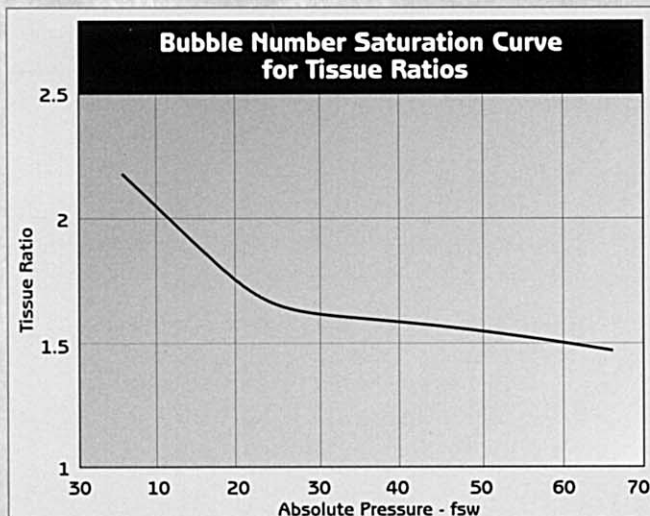
Bubble Number Saturation Curve for Tissue Ratios

Figure 11—The saturated tissue ratio, R, approaches a near constant value in both the large and small P limits in exponentially decreasing seed models, specifically in the VPM and RGBM, of the form in absolute pressure units, $R = 2.31 - \exp(-11.3/P)$, that is, 2.31 for small P and 1.31 for large P. Tissue ratios are thus bounded for all pressures.

elimination processes asymmetric. Instead of both exponential uptake and elimination, exponential uptake and linear elimination response functions can be used. Such modifications can again be employed in any perfusion model easily, and tuned to the data.

Thermodynamic Model

The thermodynamic approach suggested by Hills, and extended by others, is more comprehensive than earlier models, addressing a number of issues simultaneously, such as tissue gas exchange, phase separation, and phase volume trigger points. This model is based on phase equilibration of dissolved and separated gas phases, with temporal uptake and elimination of inert gas controlled by perfusion and diffusion. From a boundary (vascular) zone of thickness, a, gases diffuse into the cellular region. Radial, one dimensional, cylindrical geometry is assumed as a starting point, though the extension to higher dimensionality is straightforward. As with all dissolved gas transfer, diffusion is controlled by the difference between the instantaneous tissue tension and the venous tension, and perfusion is controlled by the difference between the arterial and venous tension. A mass balance for gas flow at the vascular cellular interface, a, enforces the perfusion limit when appropriate, linking the diffusion and perfusion equations directly. Blood and tissue tensions are joined in a complex feedback loop. The trigger point in the thermodynamic model is the separated phase volume, related to a set of mechanical pain thresholds for fluid injected into connective tissue.

The full thermodynamic model is complex, though Hills has performed massive computations correlating with the data, underscoring basic model validity. One of its more significant features can be seen in Figure 3. Considerations of free phase dynamics (phase volume trigger point) require deeper decompression staging formats, compared to considerations of critical tensions, and are characteristic of phase models. Full blown bubble models require the same, simply to minimize bubble excitation and growth.

Reduced Gradient Bubble Model

The reduced gradient bubble model (RGBM), developed by Wienke, treats both dissolved and free phase transfer mechanisms, postulating the existence of gas seeds (micronuclei) with permeable skins of surface active molecules, small enough to remain in solution and strong enough to resist collapse. The model is based upon laboratory studies of bubble growth and nucleation, and grew from a similar model, the varying permeability model (VPM), treating bubble seeds as gas micropockets contained by pressure permeable elastic skins

Inert gas exchange is driven by the local gradient, the difference between the arterial blood tension and the instantaneous tissue tension. Compartments with 1, 2, 5, 10, 20, 40, 80, 120, 240, 480, and 720 halftimes, τ, are again employed. While, classical (Haldane) models limit exposures by requiring that the tissue tensions never exceed the critical tensions, fitted to the US Navy nonstop limits, for example. The reduced gradient bubble model, however, limits the supersaturation gradient, through the phase volume constraint. An exponential distribution of bubble seeds, falling off with increasing bubble size is assumed to be excited into growth by compression-decompression. A critical radius, r sub c, separates growing from contracting micronuclei for given ambient pressure, P_c. At sea level, $P_c = 33$ fsw, $r_c = .8$ microns, and $\Delta P = d$. Deeper decompressions excite smaller, more stable, nuclei.

Within a phase volume constraint for exposures, a set of nonstop limits, t_n, at depth, d, satisfy a modified law, $dt_n^{1/2} = 400$ fsw min$^{1/2}$, with gradient, G, extracted for each compartment, τ, using the nonstop limits and excitation radius, at generalized depth, $d = P - 33$ fsw. Tables 2 and 3 summarize t_n, G_0, ΔG, and δ, the depth at which the compartment begins to control exposures.

Gas filled crevices can also facilitate nucleation by cavitation. The mechanism is responsible for bubble *formation occurring on solid surfaces* and container walls. In gel experiments, though, solid particles and ragged surfaces were seldom seen, suggesting other nucleation mechanisms. The existence of stable gas nuclei is paradoxical. Gas bubbles larger than 1 micron should float to the surface of a standing liquid or gel, while smaller ones should dissolve in a few seconds. In a liquid supersaturated with gas, only bubbles at the critical radius, r_c, would be in equilibrium (and very unstable equilibrium at best). Bubbles larger than the critical radius should grow larger, and bubbles smaller than the critical radius should collapse. Yet, the Yount gel experiments confirm the existence of stable gas phases, so no matter what the mechanism, effective surface tension must be zero.

Although the actual size distribution of gas nuclei in humans is unknown, these experiments in gels have been correlated with a decaying exponential (radial) distribution function. For a stabilized distribution accommodated by the body at fixed pressure, P_c, the excess number of nuclei excited by compression-decompression must be removed from the body. The rate at which gas inflates in tissue depends upon both the excess bubble number, and the supersaturation gradient, G. The critical volume hypothesis requires that the integral of the product of the two must always remain less than some volume limit point, α V, with α, a proportionality constant. A conservative set of bounce gradients, $\bar{G}$, can be also be extracted for multiday and repetitive diving, provided they are multiplicatively reduced by a set of bubble factors, η^{rep}, η^{reg}, η^{exc}, all less than one, such that $\bar{G} = \eta^{rep} \eta^{reg} \eta^{exc} G$.

These three bubble factors reduce the driving gradients to maintain the *phases volume constraint. The first* bubble factor reduces G to account for creation of new stabilized micronuclei over time scales of days. The second factor accounts for additional micronuclei excitation on deeper-than-previous dives. The third bubble factor accounts for bubble growth over repetitive exposures on time scales of hours. These repetitive, multiday, and excitation factors, η^{rep}, η^{reg}, and η^{exc}, are drawn in Figures 4, 5, and 6, using conservative parameter values. Clearly, the repetitive factors, η^{rep}, relax to one after about 2 hours, while the multiday factors, η^{reg}, continue to decrease with increasing repetitive activity, though at very slow rate. Increases in bubble elimination halftime and nuclei regeneration halftime will tend to decrease η^{rep} and increase η^{reg}. Figure 4 plots η^{rep} as a function of surface interval in minutes for the 2, 10, 40, 120, and 720 minute tissue compartments, while Figure 5 depicts η^{reg} as a function of cumulative exposure in days for 7, 14, and 21 days. The repetitive fractions, η^{rep}, restrict back to back repetitive activity considerably for short surface intervals. The multiday fractions get small as multiday activities increase continuously beyond 2 weeks. Excitation factors, η^{exc}, are collected in Figure 6 for exposures in the range 40-200 fsw. Deeper-than-previous excursions incur the greatest reductions in permissible gradients (smallest η^{exc}) as the depth of the exposure exceeds previous maximum depth. Figure 6 depicts η^{exc} for various combinations of depths, using 40, 80, 120, 160, and 200 fsw as the depth of the first dive.

Tissue Bubble Diffusion Model
The tissue bubble diffusion model (TBDM), according to Gernhardt and Vann, considers the diffusive growth of an extravascular bubble under arbitrary hyperbaric loadings. *The approach incorporates inert gas diffusion across the tissue-bubble interface, tissue elasticity, gas solubility and diffusivity, bubble surface tension, and perfusion limited transport to the tissues. Tracking bubble growth over a range of exposures, the model can be extended to oxygen breathing and inert gas switching. As a starting

point, the TBDM assumes that, through some process, stable gas nuclei form in the tissues during decompression, and subsequently tracks bubble growth with dynamical equations. Diffusion limited exchange is invoked at the tissue-bubble interface, and perfusion limited exchange is assumed between tissue and blood, very similar to the thermodynamic model, but with free phase mechanics. Across the extravascular region, gas exchange is driven by the pressure difference between dissolved gas in the tissue and free gas in the bubble, treating the free gas as an ideal. Initial nuclei in the TBDM have assumed radii near 3 microns at sea level, to be compared with .8 microns in the RGBM.

As in any free phase model, bubble volume changes become more significant at lower ambient pressure, suggesting a mechanism for enhancement of hypobaric bends, where constricting surface tension pressures are smaller than those encountered in hyperbaric cases.

As seen in Figure 7, the model has been coupled to statistical likelihood, correlating bubble size with decompression risk, a topic discussed in a few chapters. For instance, a theoretical bubble dose of 5 ml correlates with a 20% risk of decompression sickness, while a 35 ml dose correlates with a 90% risk, with the bubble dose representing an unnormalized measure of the separated phase volume. Coupling bubble volume to risk represents yet another extension of the phase volume hypothesis, a trigger point mechanism for mends incidence.

Saturation Curve

The saturation curve, relating permissible gas tension, Q, as a function of ambient pressure, P, depicted in Figure 8 for air, sets a lower bound, so to speak, on decompression staging. All staging models and algorithms must collapse to the saturation curve as exposure times increase in duration. In short, the saturation curve represents one extreme for any

staging model. Bounce curves represent the other extreme. Joining them together for diving activities in between is a model task, as well as joining the same sets of curves over varying ambient pressure ranges. In the latter case, extending bounce and saturation curves to altitude is just such an endeavor.

Models for controlling hypobaric and hyperbaric exposures have long differed over range of applicability. Recent analyses of very high altitude washout data question linear extrapolations of the hyperbaric saturation curve, Figure 8, to hypobaric exposures, pointing instead to correlation of data with constant decompression ratios in animals and humans. Correlations of hypobaric and hyperbaric data, however, can be effected with a more general form of the saturation curve, one exhibiting the proper behavior in both limits. Closure of hypobaric and hyperbaric diving data can be managed with one curve, exhibiting linear behavior in the hyperbaric regime, and bending through the origin in the hypobaric regime. Using the RGBM and a basic experimental fact that the number of bubble seeds in tissue increase exponentially with decreasing bubble radius, just such a single expression can be obtained. The limiting forms are exponential decrease with decreasing ambient pressure (actually through zero pressure), and linear behavior with increasing ambient pressure. Accordingly, Figures 9, 10, and 11 exhibit Q, G, and R as a function of P for the expression (in terms of parameters ζ and ξ. Asymptotic forms are quite evident. Such general forms derive from the RGBM, depending on a coupled treatment of both dissolved and free gas phases. Coupled to the phase volume constraint, these models suggest a consistent means to closure of hypobaric and hyperbaric data.

The Abyss RGBM Implementation

As of this writing the only commercially available decompression software that incorporates the reduced gradient bubble model (RGBM) is Abyss. The RGBM is a dual phase (dissolved and free gas) algorithm for diving calculations. Incorporating and coupling historical Haldanean dissolved gas transport with bubble excitation and growth, the RGBM extends the range of computational applicability of traditional methods. The RGBM is correlated with diving and exposure data on more complete physical principles. Much is new in the RGBM algorithm, and troublesome multidiving profiles with higher incidence of DCS are a target here. Some highlighted extensions for the ABYSS implementation of the Buhlmann basic algorithm include:

❑ Restricted repetitive exposures, particularly beyond 100 ft, based on reduction in permissible bubble diffusion gradients within 2 hr time spans;
❑ Restricted yo-yo and spike (multiple ascents and descents) dives based on excitation of new bubble seeds;
❑ Restricted deeper-than-previous dives based on excitation of very small bubble seeds over 2 hr time spans:
❑ Restricted multiday diving based on adaptation and regrowth of new bubble seeds;
❑ Smooth coalescence of bounce and saturation limit points using 32 tissue compartments;
❑ Consistent treatment of altitude diving, with proper zero point extrapolation of limiting tensions and permissible bubble gradients (through zero as pressure approaches zero);
❑ Algorithm linked to diving data (tests), Doppler bubble, and laboratory micronuclei experiments;
❑ Additional parameters reducing exposure time accounting for fitness, work load, and water temperature. 👍

Dr. Bruce Weinke holds Bachelors Degrees in Physics and Mathematics, a Masters Degree in Nuclear Physics, and a PdD in Particle Physics. He is the Director of the Computational Testbed for Industry at the Los Alamos Advanced Computing Laboratory in New Mexico. He is a former U.S. Navy SEAL, a NAUI Instructor Trainer, a PADI Master Instructor, and a YMCA Institute Director. He is a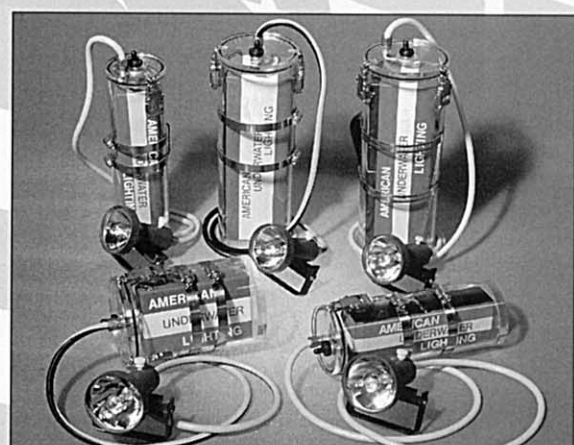lso active in Professional Ski Racing and Ski Race Coaching.